Effect of structural anisotropy on the coarsening kinetics of diblock copolymer striped patterns

R. Ruiz,[1,*] J. K. Bosworth,[2] and C. T. Black[1,†]
[1]*IBM Thomas J. Watson Research Center, Yorktown Heights, New York 10598, USA*
[2]*Department of Materials Science and Engineering, Cornell University, Ithaca, New York 14853, USA*
(Received 24 October 2007; published 29 February 2008)

We compare the time evolution of striped pattern correlation lengths for three different poly(styrene-*b*-methyl methacrylate) (PS-*b*-PMMA) diblock copolymer materials having comparable molecular diffusion rates. Striped patterns formed from cylindrical-phase materials coarsen with enhanced growth exponents and have reduced disclination diffusion activation energies as compared to striped patterns formed from smectic A lamellar-phase materials. The observed differences stem from distinct topological constraints in cylindrical (columnar) and lamellar (SmA) striped patterns. Cylindrical domains create a channel for layer breaking without molecule interdiffusion, facilitating an enhanced rate of pattern coarsening and reducing the disclination diffusion activation energy.

DOI: 10.1103/PhysRevB.77.054204 PACS number(s): 61.72.Lk, 83.80.Uv, 68.35.Fx, 81.16.Rf

I. INTRODUCTION

Pattern coarsening in block copolymers is ultimately the result of the collective motion of molecules toward an equilibrium configuration. Microscopic diffusion of individual molecules translates into defect motion and annihilation, which manifests as a macroscopic pattern coarsening effect. Numerous studies have separately examined both pattern coarsening[1–7] and molecular diffusion mechanisms;[8–15] however, there is currently no formal link connecting both phenomena. Coarsening of striped patterns formed by diblock copolymer materials involves multiple defect annihilation events that can be strongly suppressed when topology and molecular diffusion anisotropy inhibit layer breaking.

In this paper, we compare the time evolution of striped pattern correlation lengths for three different poly(styrene-*b*-methyl methacrylate) (PS-*b*-PMMA) materials having largely comparable molecular diffusion rates. Despite this material similarity, we measure enhanced pattern coarsening and a correspondingly reduced disclination diffusion activation energy in a cylindrical-phase PS-*b*-PMMA material as compared to two lamellar materials of smaller molecular weight, strongly suggesting that topological differences in the material film structure play a key role in the dynamics of pattern formation. We use the distinctive growth exponents measured for each system to establish a connection between molecular diffusion anisotropy and macroscopic pattern scaling behavior.

II. EXPERIMENTAL DETAILS

We form striped patterns from thin films of both perpendicularly oriented lamellar-phase [Figs. 1(a)–1(c)] and parallel-oriented cylindrical-phase PS-*b*-PMMA diblock copolymers [Figs. 1(d)–1(f)] by spin casting from dilute solutions to a film thickness equal to the characteristic domain spacing L_0 for each material. The lamellar striped pattern results from a layered molecular arrangement that corresponds to a smectic A (SmA) liquid crystal.[16] The director, a unit vector defining the local order parameter, points perpendicular to the stripes. The cylindrical-phase material arranges in a hexagonal columnar pattern and a striped pattern forms from a plane containing a single layer of cylinders. For computational purposes, we define the director as being oriented perpendicular to the long cylinder axis and lying in the cylinder plane, even though, in fact, the molecule layering is circular around the cylinder axis. We studied two different lamellar-phase materials, *Lam32* (average number molecular weight M_n=32 kg/mol, polystyrene (PS) weight fraction f=0.5, atactic polymethyl methacrylate (PMMA) content, polydispersity index PDI=1.11) with L_0=22 nm and *Lam46* (M_n=46 kg/mol, f=0.5, rich in syndiotactic PMMA content, PDI=1.08) with L_0=32 nm, and one cylindrical-phase material, *Cyl64* (M_n=64 kg/mol, f=0.66, atactic PMMA content, PDI=1.16) with L_0=37 nm. Forming striped patterns in perpendicularly oriented lamellar materials (*Lam32* and *Lam46*)

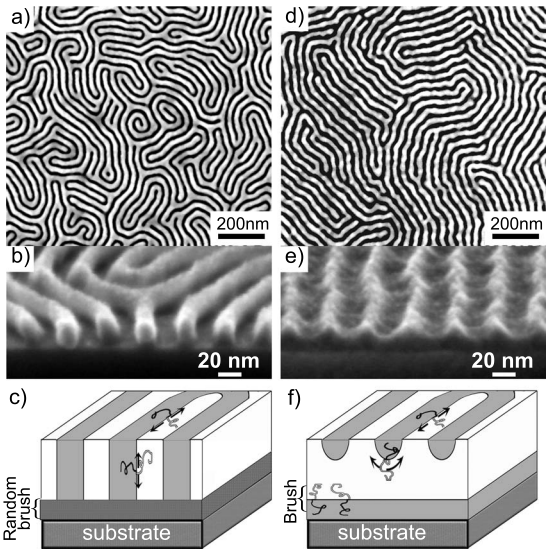

FIG. 1. Striped patterns from lamellar (left) and cylindrical (right) thin films: [(a) and (d)] top down scanning electron microscopy (SEM) of striped patterns, [(b) and (e)] cross section SEM after PMMA removal, and [(c) and (f)] cross section schematic of molecular arrangement showing possible directions for parallel diffusion (D_{par}).

requires first creating a neutral wetting surface using a PS-*r*-PMMA random copolymer[17] [Figs. 1(a)–1(c)]. For *Cyl64*, PMMA preferential wetting of the silicon oxide surface[18] forms a monolayer brush, and polymer molecules self-organize on top of the brush into a single layer of surface-parallel PMMA cylinders embedded in a PS matrix [Figs. 1(d)–1(f)]. We observed the striped pattern time evolution by annealing for times ranging from 10 to 4000 min at temperatures (T) between 180 and 220 °C.

III. COARSENING IN CYLINDRICAL AND LAMELLAR DIBLOCK COPOLYMER STRIPED PATTERNS

Diblock copolymer striped patterns coarsen with annealing time according to a power law,[2,5,19,20]

$$\xi(t) = A_T t^{\phi}, \quad t > t_0, \tag{1}$$

where $\xi(t)$ is the correlation length at time t and ϕ is called the growth exponent. Here, A_T is a T-dependent coefficient that can be expressed dimensionally as $A_T = \xi_{0T}/t_0^{\phi}$, where t_0 is an initial time on the order of the microphase separation time and $\xi_{0,T}$ is the initial correlation length at t_0 and temperature T.

The growth exponent (ϕ) is not universal for diblock copolymer striped patterns, as patterns formed by these three PS-*b*-PMMA materials all coarsen differently with annealing time (Fig. 2). We measured the striped pattern correlation length by computing the order parameter using a previously described procedure.[21] We extracted ϕ from plots of ξ versus annealing time for the three materials at different annealing T according to Eq. (1) (Fig. 2 shows data for $T=180$ and 210 °C, plots for $T=195$ and 220 °C are not shown, and data for *Lam46* and *Cyl64* at 195° can be found elsewhere[21]). For a given material, ϕ remains constant over the T range of these measurements. Films of the two lamellar materials *Lam32* and *Lam46* coarsen slowly with time over the measured T range ($\phi \approx 0.14$ and $\phi \approx 0.02$, respectively), while patterns formed from the cylindrical *Cyl64* show a significantly larger growth exponent ($\phi \approx 0.26$). We rule out differences caused by pinning effects associated with the different underlying polymer brushes (i.e., the PS-*b*-PMMA brush for *Cyl64* and the PS-*r*-PMMA brush for *Lam32* and *Lam46*), as previous measurements of perpendicularly oriented PS-*b*-PMMA cylindrical domains using the same PS-*r*-PMMA brush yielded $\phi=0.25$, similar to that of *Cyl64* (Ref. 3) supporting the notion that the choice of brush is not the cause for a different coarsening exponent.

Coarsening in block copolymer striped patterns occurs by defect motion and annihilation, processes that ultimately involve diffusion of individual polymer molecules. The defect motions considered here occur by either climb or glide mechanisms.[1,7,16,22] Climb describes a dislocation displacement in the plane of the layers, perpendicular to the Burgers vector. Climb occurs by collective diffusion of molecules parallel to the striped layers in both lamellar [Fig. 1(c)] and cylindrical [Fig. 1(f)] patterns. Glide describes defect motion perpendicular to the plane of the striped pattern layers and inevitably requires layer breaking. In the SmA lamellar phase, at the molecular level,[7] glide necessarily involves interdiffusion across domain boundaries [Fig. 1(c)], a highly unfavorable process due to the enthalpic penalty for block mixing.[23] In the columnar phase, layer breaking can be achieved by either molecular interdiffusion or *by utilizing the interconnectivity of the embedding matrix* to diffuse around the cylinder core [Fig. 1(f)].

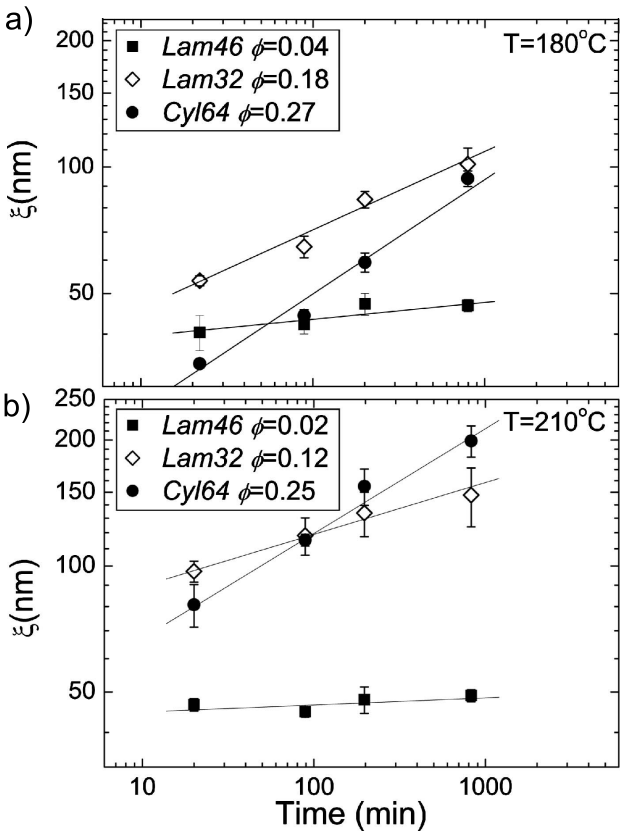

FIG. 2. Striped pattern correlation length versus annealing time for *Lam46*, *Lam32*, and *Cyl64* block copolymer thin films. (a) Annealing at $T=180$ °C and (b) annealing at $T=210$ °C.

IV. ACTIVATION ENERGIES

In the following analysis, we use growth exponent measurements as a first attempt to link pattern evolution to molecular diffusion. The correlation length (ξ) is proportional to the average separation distance between defects disrupting orientational order (i.e., disclinations). The time-dependent disclination density $\rho(t)$ is given by[5]

$$\rho(t) \sim \xi^{-2}(t). \tag{2}$$

Pattern defects introduce stress fields that generate an attractive force between defects of opposite sign (the Peach-Koehler force). When these stress fields are large enough to overcome layer compression, defects move and approach each other in a process that involves layer breaking and consequent creation and annihilation of elementary edge dislocations.[5,16,22,24]

To relate measurements of striped pattern correlation lengths to the activation energy for defect diffusion, we first

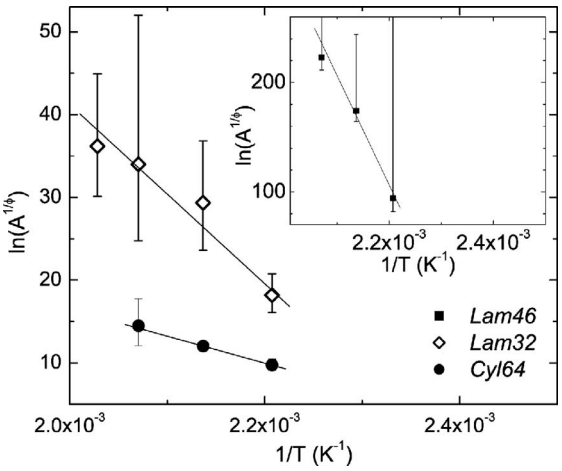

FIG. 3. Activation energy. $\ln(A^{1/\phi})$ versus $1/T$ for *Lam32* (open diamonds, E_a=900 kJ/mol) and for *Cyl64* (solid circles, E_a=270 kJ/mol). Inset: *Lam46* (solid squares, E_a=8300 kJ/mol).

make a simplifying assumption that defects disrupting orientational order all move with the same velocity $v(t)$. Because the average distance between defects is proportional to $\xi(t)$, the disclination velocity at a given time t is proportional to the rate of change in correlation length,

$$v(t) \sim \frac{d\xi(t)}{dt} = \phi\frac{\xi(t)}{t}, \tag{3}$$

where $\xi(t)$ is given by Eq. (1). Expressed in terms of defect density ρ, Eq. (3) becomes

$$v(\rho) \sim \phi A_T^{1/\phi}\rho^{(1-\phi/2\phi)}. \tag{4}$$

Defect motion in striped patterns is analogous to vacancy or interstitial diffusion in solid crystals[16] and therefore we expect a thermally activated behavior [i.e., $v(t)\sim\exp(-E_a/kT)$]. We can determine this activation energy E_a by evaluating the dislocation speed (v) at a constant defect density (i.e., at fixed defect separation distance) as a function of T,

$$v(\rho=\rho_{const},T) \sim \left.\phi A_T^{1/\phi}\rho^{(1-\phi/2\phi)}\right|_{\rho=\rho_{const}} = Ce^{-E_a/kT}, \tag{5}$$

$$\ln(A_T^{1/\phi}) = -\frac{E_a}{kT} + \text{const}. \tag{6}$$

Equations (5) and (6) are valid if ϕ is independent of T, which is true for the range of measurements in our experiments [Fig. 2] as well as in other block copolymer thin films.[1]

To evaluate the defect diffusion activation energy (E_a) for the three PS-*b*-PMMA materials, at each T, we use Eq. (1) to determine both the corresponding ϕ and the coefficient A_T. With these values, we generate an Arrhenius plot (Fig. 3) to estimate E_a using Eq. (6). We measure E_a for *Cyl64* of 270 kJ/mol; it is more than three times smaller than that of either lamellar-phase pattern where E_a=900 kJ/mol for *Lam32* and $E_a>8300$ kJ/mol for *Lam46*. Our estimated E_a for *Cyl64* compares well with previous measurements of 377 kJ/mol for disclination diffusion in cylindrical films of PS-*b*-PMMA with M_n=84 kg/mol,[25] while E_a for lamellar patterns has never been measured. The error bars in Fig. 3 result from propagating the uncertainty in ϕ (from the linear fits in Fig. 2) to $\ln(A_T^{1/\phi})$. We have omitted T=220 °C data for *Cyl64* because the material showed signs of thermal decomposition. For *Lam46*, experimental uncertainty in the small values of ϕ causes the error bars in $\ln(A_T^{1/\phi})$ to diverge, as would be the case in a system having an infinite activation energy. Therefore, we interpret the estimated value for *Lam46* (8300 kJ/mol) as a lower bound for E_a. The enhanced ϕ and lower activation energy of the cylindrical-phase striped pattern (as compared to lamellar-phase striped patterns) show that defect dynamics are not universal across all striped pattern systems and are influenced by topological factors.

V. MOLECULAR DIFFUSION AND STRUCTURAL ANISOTROPY

Collective molecular diffusion lies at the heart of striped pattern defect dynamics. In microphase separated systems, molecular diffusion *along* microdomains (i.e., parallel to the pattern stripes) is favored over diffusion *across* domains because of the enthalpic penalty of block mixing.[8,9,13,23,26] For nonentangled block copolymers, the parallel (D_{par}) and perpendicular (D_{perp}) diffusion constants are[13,26]

$$D_{par} \approx D_0,$$

$$D_{perp} \sim D_0 e^{-\alpha\chi N_A}, \tag{7}$$

where $D_0=(k_BT/N\zeta)$ is the Rouse model diffusion constant,[27] α is a material parameter of order unity,[26,28] N_A is the degree of polymerization of the block infiltrating the unfavorable domain,[26] and ζ is a monomeric friction factor. The exponential factor χN_A is responsible for the diffusion anisotropy.[11,13] Estimating $\alpha\approx1$, we calculate $D_{perp}/D_0 \sim 10^{-3}-10^{-4}$ for all three, *Cyl64*, *Lam32*, and *Lam46*, materials (see Table I). In a SmA phase (i.e., lamellar), defect annihilation requires layer breaking, meaning molecular diffusion across domains with diffusion constant D_{perp}. We understand the faster coarsening kinetics of SmA *Lam32* (ϕ=0.14) as compared to *Lam46* (ϕ=0.02) as originating from the lower molecular weight (*Lam32*) having a higher rate of perpendicular diffusion events [Eq. (7)] and a correspondingly higher rate of defect annihilation. The *Cyl64* striped pattern coarsens *faster than either lamellar material* (ϕ=0.26) despite having the highest molecular weight such that the factor χN_A (and thus D_{perp}) is approximately equal to that of *Lam42*—the material that does not coarsen appreciably (Table I). We note that polymer entanglement cannot account for the observed difference in pattern coarsening rates. Chain entanglement occurs above a critical molecular weight M_c, which is ~35 kg/mol for PS[29] and ~30 kg/mol for PMMA,[29] so that the only slightly entangled block in our experiments is the PS block in *Cyl64* ($M_{n\text{PS}}$ =42 kg/mol)—the material having the *fastest* coarsening kinetics in our experiments.

TABLE I. Material parameters for the three block copolymers used in this experiment. M_n= Number average molecular weight. f=PS volume fraction. N=degree of polymerization of the PS or PMMA block. D_0=self-diffusion constant at 200 °C (estimate). ϕ=average value for the growth exponent. E_a=defect diffusion activation energy. χ=Flory Huggins parameter ($\chi=0.028+3.9/T$) (Ref. 31). $\exp(-\chi^* N_A)$ =diffusion anisotropy estimated at 200 °C. D_0 for *Lam32* and *Cyl64* were calculated using a monomeric friction coefficient for atactic PMMA, while syndiotactic PMMA was assumed for *Lam46* (Ref. 29).

Material	M_n (kg/mol)	f	N (PS)	N (PMMA)	D_0 cm^2/s	ϕ	E_a (kJ/mol)	$\chi^* N$ (at 200 °C)	$\chi^* N_A$ (at 200 °C)	$\exp(-\chi^* N_A)$
Lam32	32.3	0.5	155.3	161.5	2.55×10^{-12}	0.14	900	11.5	5.9	2.87×10^{-03}
Lam46	45.9	0.48	211.8	238.7	5.46×10^{-13}	0.02	8300	16.3	8.7	1.75×10^{-04}
Cyl64	64	0.66	406.2	230.4	1.79×10^{-12}	0.26	270	23.1	8.4	2.36×10^{-04}

We believe that the enhanced coarsening kinetics of the cylindrical striped pattern stems from the fundamental topological difference between the two phases. Even though SmA and columnar phases form similar striped patterns, structural differences between a two-dimensional lamellar profile and a cylindrical columnar structure surrounded by an embedding matrix give rise to differences in the distribution of compressional stresses around defect structures.[16,22] In cylindrical-phase patterns, an individual polymer molecule diffusing parallel to the domain interface can move with components that are perpendicular and parallel to the director by moving either parallel to the cylinder axis or alternatively *rotating around the cylinder core*; the diffusion constant associated with both these motions is D_{par} (Fig. 1), as neither involves domain traversal. Molecular motion around cylinder cores opens a channel for layer breaking *without perpendicular diffusion* in columnar-phase materials, in contrast to lamellar phases where D_{par} is associated only with motion perpendicular to the director, that is, parallel to striped domains or vertically along lamellae walls (Fig. 1). We note that the origin of the difference in pattern coarsening is the interconnected matrix present in cylindrical-phase materials, consistent with previous observations of apparent increased diffusion rates in systems having interconnecting paths[13,26] and also consistent with recent *in situ* microscopy measurements[30] of cylindrical-phase patterns, where diffusion values estimated from the driving force of a "closing connection" (i.e., layer breaking) were about 3 orders of magnitude higher than the "expected" D_{perp}, that is, comparable to D_{par}. We believe that the observed growth exponent of $\phi\approx\frac{1}{4}$ in other cylindrical[3,5,21] and spherical[2] block copolymer phases represents a limiting case for nonentangled polymers having an interconnecting matrix, while lower growth exponents result from patterns lacking an embedding matrix or having highly entangled chains.

At short annealing times, striped patterns formed from the lower molecular weight, *Lam32*, show larger ξ than either *Lam46* or *Cyl64*. The initial correlation length ($\xi_{0,T}$) is largely determined by the diffusion constant D_0, which characterizes the molecular diffusivity prior to pattern microphase separation. In PS-*b*-PMMA materials, D_0 is limited by the PMMA block ($\zeta_{PMMA}/\zeta_{PS}\sim10^3$) (Ref. 29) and so we estimate D_0 (Table I) between $\sim0.5\times10^{-12}$ and 3×10^{-12} cm^2/s for all three materials (assuming ζ in the block copolymer material stays relatively unchanged with respect to its homopolymer value). Note that *Lam46* and *Cyl64* have similar PMMA content and thus similar D_0. D_0 is slightly larger for *Lam32* than for the two other materials because of its lower degree of polymerization N, resulting in a larger $\xi_{0,T}$. The effect of $\xi_{0,T}$ can be appreciated qualitatively from the y intercepts in Fig. 2. Although initially *Lam32* has a larger ξ due to a higher D_0, the pattern coarsens only slowly with time such that eventually ξ of *Cyl64* surpasses that of the *Lam32* material. The time at which this crossover occurs shortens with increasing T from about 2000 min at 180 °C to as short as 10 min at 220 °C.

VI. CONCLUSIONS

We have measured significantly different scaling behaviors in striped patterns formed from diblock copolymer materials having substantially similar molecular diffusivities—an observation we attribute directly to topological differences between material systems. Striped patterns formed from SmA lamellar-phase materials (*Lam32* and *Lam46*) coarsen slowly with time ($\phi=0.14$ and $\phi=0.02$, respectively) and have disclination diffusion activation energies of 900 and >8300 kJ/mol, respectively. Striped patterns formed of higher molecular weight cylindrical-phase materials (*Cyl64*) coarsen faster with time ($\phi=0.26$) with lower defect diffusion activation energy (270 kJ/mol). The topological difference between cylindrical (columnar) and lamellar (SmA) striped patterns creates a channel for layer breaking in cylindrical patterns without molecule interdiffusion, facilitating an enhanced rate of pattern coarsening and reducing defect annihilation activation energy.

ACKNOWLEDGMENT

The authors thank G. Breyta (IBM Almaden) for synthesizing some of the diblock copolymers used in this work.

*Present address: Hitachi Global Storage Technologies, San Jose Research Center, San Jose, CA 95125.
†Present address: Brookhaven National Laboratory, Center for Functional Nanomaterials, Upton, NY 11973.

[1] C. Harrison, Z. Cheng, S. Sethuraman, D. A. Huse, P. M. Chaikin, D. A. Vega, J. M. Sebastian, R. A. Register, and D. H. Adamson, Phys. Rev. E **66**, 011706 (2002).
[2] C. Harrison, D. E. Angelescu, M. Trawick, Z. D. Cheng, D. A. Huse, P. M. Chaikin, D. A. Vega, J. M. Sebastian, R. A. Register, and D. H. Adamson, Europhys. Lett. **67**, 800 (2004).
[3] C. T. Black and K. W. Guarini, J. Polym. Sci., Part A: Polym. Chem. **42**, 1970 (2004).
[4] R. A. Segalman, A. Hexemer, and E. J. Kramer, Phys. Rev. Lett. **91**, 196101 (2003).
[5] C. Harrison, D. H. Adamson, Z. Cheng, J. M. Sebastian, S. Sethuraman, D. A. Huse, R. A. Register, and P. M. Chaikin, Science **290**, 1558 (2000).
[6] K. Amundson, E. Helfand, X. Quan, and S. D. Smith, Macromolecules **26**, 2698 (1993).
[7] K. Amundson, E. Helfand, X. Quan, S. D. Hudson, and S. D. Smith, Macromolecules **27**, 6559 (1994).
[8] K. R. Shull and E. J. Kramer, Macromolecules **24**, 1383 (1991).
[9] D. Ehlich, M. Takenaka, S. Okamoto, and T. Hashimoto, Macromolecules **26**, 189 (1993).
[10] M. C. Dalvi and T. P. Lodge, Macromolecules **26**, 859 (1993).
[11] T. P. Lodge and M. C. Dalvi, Phys. Rev. Lett. **75**, 657 (1995).
[12] G. Fleischer, F. Rittig, S. Stepanek, K. Almdal, and C. M. Papadakis, Macromolecules **32**, 1956 (1999).
[13] M. W. Hamersky, M. A. Hillmyer, M. Tirrell, F. S. Bates, T. P. Lodge, and E. D. von Meerwall, Macromolecules **31**, 5363 (1998).
[14] P. F. Green, T. P. Russell, R. Jerome, and M. Granville, Macromolecules **21**, 3266 (1988).
[15] C. M. Papadakis and F. Rittig, J. Phys.: Condens. Matter **17**, R551 (2005).
[16] M. Kleman and O. D. Lavrentovich, *Soft Matter Physics. An Introduction* (Springer-Verlag, New York, 2003).
[17] P. Mansky, Y. Liu, E. Huang, T. P. Russell, and C. Hawker, Science **275**, 1458 (1997).
[18] S. H. Anastasiadis, T. P. Russell, S. K. Satija, and C. F. Majkrzak, Phys. Rev. Lett. **62**, 1852 (1989).
[19] D. Boyer and J. Vinals, Phys. Rev. E **64**, 050101 (2001).
[20] A. J. Bray, Adv. Phys. **43**, 357 (1994).
[21] R. Ruiz, R. L. Sandstrom, and C. T. Black, Adv. Mater. (Weinheim, Ger.) **19**, 587 (2007).
[22] P.-G. De Gennes and J. Prost, *The Physics of Liquid Crystals* (Oxford University Press, Oxford, 1993).
[23] M. C. Dalvi, C. E. Eastman, and T. P. Lodge, Phys. Rev. Lett. **71**, 2591 (1993).
[24] L. Tsarkova, A. Horvat, G. Krausch, A. V. Zvelindovsky, G. J. A. Sevink, and R. Magerle, Langmuir **22**, 8089 (2006).
[25] J. Hahm and S. J. Sibener, J. Chem. Phys. **114**, 4730 (2001).
[26] K. A. Cavicchi and T. P. Lodge, Macromolecules **37**, 6004 (2004).
[27] M. Doi and S. F. Edwards, *The Theory of Polymer Dynamics* (Oxford University Press, Oxford 1986).
[28] H. Yokoyama and E. J. Kramer, Macromolecules **31**, 7871 (1998).
[29] J. D. Ferry, *Viscoelastic Properties of Polymers* (Wiley, New York, 1980).
[30] L. Tsarkova, A. Knoll, and R. Magerle, Nano Lett. **6**, 1574 (2006).
[31] T. P. Russell, R. P. Hjelm, Jr., and P. A. Seeger, Macromolecules **23**, 890 (1990).